First-principles study of filled and unfilled skutterudite antimonies

Marek Veithen and Philippe Ghosez
Département de Physique, Université de Liège, B-5, B-4000 Sart-Tilman, Belgium
(Dated: February 2, 2008)

The electron localization tensor, Born effective charges, dielectric constants and phonon dispersion relations of the skutterudite $CoSb_3$ and the filled skutterudite $TlFeCo_3Sb_{12}$ have been studied using density functional perturbation theory. The origin of the low energy peak in the phonon density of states of $TlFeCo_3Sb_{12}$ observed recently by Neutron inelastic scattering [R. P. Hermann *et al.*, Phys. Rev. Lett. **90**, 135505 (2003)] is attributed to the vibrations of Tl that show only weak coupling with the normal modes of the host crystal. Moreover, the dielectric properties of these materials show unsual features such as giant Born effective charges and a strong increase of the optical and static dielectric tensor in the filled compound.

PACS numbers: 63.20.Dj,77.22.-d,71.15.Mb

I. INTRODUCTION

$CoSb_3$ belongs to the class of binary skutterudites[1]. These materials are characterized by a complex cristalline structure containing large voids and four formula units per cell. It has been observed that filling the voids with electropositive atoms such as Tl or rare earth atoms leads to a drastic decrease of the lattice thermal conductivity[2,3]. Combined with good semiconducting properties (electrical conductivity, Seebeck coefficient), this makes the so-called filled skutterudites potentially interesting for thermoelectric applications such as refrigeration or energy generation[4].

One mechanism that has been evoked to explain the strong reduction of the lattice thermal conductivity in filled skutterudites is a strongly anharmonic rattling motion of the filling atom. Keppens and co-workers[5] used inelastic neutron scattering to measure the phonon density of states (DOS) of the La atoms in $LaFe_4Sb_{12}$. They found a well defined peak at about 56 cm^{-1} and a somewhat broader structure around 121 cm^{-1} that were associated to two La-dominated localized modes. Feldman and co-workers[6] used a force constant model fitted from first-principles calculations to compute the phonon dispersion relations and DOS of $LaFe_4Sb_{12}$ and $CeFe_4Sb_{12}$. Their results allowed them to refute the hypothesis of an anharmonic rare-earth potential and to suggest that the two peaks in the La projected DOS are not associated to two localized modes but are the results of hybridizations between the rare-earth and Sb vibrations.

In several respects, we can expect the behaviour of Tl to be different from that of La and Ce. First, the 4f valence states of the rare earth atoms strongly hybridize with the transition metal d and Sb p states in the vicinity of the Fermi energy[8]. These hybridizations are absent in case of Tl where the 4f states are much lower in energy. Second, the electronegativity of Tl is significantly higher than that of La and Ce and close to that of Sb. This suggests that Tl may have a smaller effect on the electrical transport properties of $CoSb_3$ than the rare-earths. Finally, the ionic radius of Tl is significantly larger than that of La or Ce. We can therefore expect the dynamical properties of Tl to be significantly different from that of the rare earths.

Some evidence of a different behaviour of Tl can be found in a recent work of Hermann and co-workers[9] who measured the phonon DOS of various Tl-filled skutterudites. These authors found a single peak arount 40 cm^{-1}, in striking difference with the two peaks of the La-filled compound.

Motivated by this work[9], we use first-principles calculations to study the lattice dynamics and dielectric properties of $CoSb_3$ and $TlFeCo_3Sb_{12}$. We show that Tl is in a harmonic potential well up to large displacements. Moreover, the peak about 40 cm^{-1} in the phonon DOS of the filled compound is due to the vibrational motion of Tl that shows only modest hybridizations whith the normal modes of the host crystal. Our calculations also confirm the existence of a single Tl-dominated peak in the DOS of the filled compound. In addition, we observe unusual dielectric porperties in $CoSb_3$ and $TlFeCo_3Sb_{12}$ such as giant Born effective charges, or a strong increase of the static dielectric constant in the filled compound. To our knowledge, this is the first first-principles study of Tl-filled skutterudites and the first time Born effective charges and dielectric constants have been computed from first-principles for these compounds.

Our paper is organized as follows. Sec. II contains the technical details of our calculations. In Sec. III, we discuss the structural and electronic properties of $CoSb_3$ and $TlFeCo_3Sb_{12}$. In Sec. IV, we discuss their optical dielectric constant and effective charges. In Sec. V, we report the zone-center phonons in the filled and unfilled compound and deduce their static dielectric tensor and infrared reflectivity. Finally, in Sec. VI, we discuss the phonon dispersion relations and DOS of $CoSb_3$ and $TlFeCo_3Sb_{12}$.

II. TECHNICAL DETAILS

Our calculations have been performed within the local density approximation to density functional theory (DFT)[10,11] thanks to the ABINIT[12] package. We worked

at the experimental lattice constant. The atomic positions have been relaxed until the forces on the atoms were smaller than $5 \cdot 10^{-5}$ hartree/bohr. For the exchange-correlation energy, we used the parametrization of Perdew and Wang[13]. The valence states were computed non-relativistically. The all-electron potentials were replaced by norm-conserving pseudopotentials generated from scalar relativistic all-electron calculations of the free atoms thanks to the FHI98PP code[14]. The Sb potential has been generated according to the Troullier-Martins scheme[15]. In order to obtain smooth pseudopotentials for Fe, Co and Tl we used the Hamann[16] scheme for these elements. The parameters used to generate the pseudopotentials are summarized in Table I. The electronic wavefunctions have been expanded in a plane wave basis. With the pseudopotentials described above a kinetic energy cutoff of 25 hartree was enough to obtain well converged results.

The static ionic charges of Sec. IV B have been computed following Bader's prescription for the partitioning of space into atomic bassins[17] as it is described in Ref. 18.

For the phonon frequencies, a $2 \times 2 \times 2$ grid of special k-points[19] was sufficient to obtain well converged results while the Born effective charges, dielectric tensors and localization tensors required a grid of $4 \times 4 \times 4$ special k-points. In fact, for the smaller grid, the violation of the charge neutrality for the Born effective charges[20] was quite important (0.2 a. u.). Using the larger grid, this error could be reduced by a factor of 10 while the phonon frequencies changed by less than 3 cm^{-1}.

The phonon frequencies, Born effective charges, localization tensors and dielectric tensors have been computed from a linear response approach to DFT[20,21,22]. The first-order derivatives of the wavefunctions have been calculated by minimizing a variational expression of the second-order energy derivatives within the parallel gauge. In order to perform the band-by-band decomposition of various quantities such as the localization tensor or the optical dielectric tensor, these wavefunctions were further transformed to the diagonal gauge[23]. We computed the dynamical matrix explicitely on a $2 \times 2 \times 2$ grid of special q-points. To obtain the full phonon band structure and DOS, we used a Fourier interpolation that includes the long range dipole-dipole interactions[24]. The lattice specific heat has been computed from the DOS as it is described in Ref. 25. This approach is more reliable than the one used in the previous studies of Singh and co-workers[6,7,26]. In Refs. 26 and 6, these authors used an empirical force constant model that had been adjusted throught LDA total energy calculations while in Ref. 7, they computed the interatomic force constants for zone-center atomic displacements only.

III. GROUND-STATE PROPERTIES

A. Crystal structure

The structure of $CoSb_3$ is formed by a bcc lattice [space group $Im\overline{3}$, lattice constant a = 9.0385 Å] with 4 formula units per primitive unit cell. It can be described as a distorted perovskite[1] with the chemical formula ABO_3. In $CoSb_3$, the site of the A atoms is empty, the sites of the B atoms are occupied by Co and the positions of O by Sb. The $CoSb_6$ octaedra are tilted so that the Sb atoms form rectangular Sb_4 rings. The Co and Sb atoms occupy respectively the 8c $(\frac{1}{4}, \frac{1}{4}, \frac{1}{4})$ and 24g $(0, y, z)$ Wyckoff positions. The relaxed values of $y = 0.33284$ and $z = 0.15965$ are in exellent agreement with the experimental results[27] of $y = 0.33537$ and $z = 0.15788$.

In the unfilled compound, the 2a $(0, 0, 0)$ Wyckoff positions are empty. They are at the centers of large voids surrounded by 12 Sb and 8 Co atoms. These voids are able to accomodate an electropositive filler such as Tl or various rare earth atoms. The electronic configuration of Tl is $6s^2\ 6p^1$. In order to fill an important fraction x of voids, all chemical bonds must be saturated. Therefore, one has to compensate the excess charge due to the Tl 6p electrons by replacing for example one Co per cell by Fe or one Sb by Sn[3].

Experimentally, the lattice constant of Tl-filled $CoSb_3$ is found to increase linearly with the amount of filled voids[3] for $0 < x < 0.8$. In our calculation, we worked at $x = 1$ and we replaced one Co per cell by Fe. We chose a lattice constant of 9.1276 Å that corresponds to a linear extrapolation of the data of Ref. 3 to $x = 1$. This choice is further justified by the fact that the residual stress in the filled compound ($2.7 \cdot 10^{-4}$ Ha/bohr^3) is similar to the stress in the unfilled compound ($2.5 \cdot 10^{-4}$ Ha/bohr^3). The relaxed reduced atomic coordinates in $TlFeCo_3Sb_{12}$ and $CoSb_3$ differ by less than 0.003.

Due to the use of periodic boundary conditions, the Fe atoms occupy the same crystallographic site in each cell. This situation is somewhat artificial since it neglects any disorder introduced by the random substitution of Co by Fe in real samples. However, we expect the lack of disorder in our calculations to have only modest effects on the electronic and dynamical properties of Tl for the Fe-compensated compound. It might be more important for other compensations such as the substituaion of Sb by Sn. First, Fe can only occupy four equivalent sites per cell while there are 12 sites that can accomodate Sn. Second, the distance between Tl and Sb (3.3897 and 3.3977 Å) is smaller than the distance between Tl and Co (3.9823 Å). Finally, we will see in Sec. VI that the vibrations of Co/Fe are strongly decoupled from the vibrations of Tl and located in the high energy region above 200 cm^{-1} of the phonon spectrum. At the opposite, the vibrations of Sb occupy the region below 200 cm^{-1} and show significant interactions with the vibrations of Tl.

TABLE I: Parameters used to generate the pseudopotentials of Fe, Co, Sb and Tl. Reported is the type of the pseudopotential (H = Hamann, TM = Troullier-Martins), the projector that is used as local component, the cutoff radii (bohr) of the s, p, d and f channels (in case they have been included in the pseudopotential) and the cutoff radius (bohr) of the partial core density (r_{nlc}). The values in brackets indicate the reference energy (eV) that has been used to build the pseudo-wavefunction in case we did not use the default value of the FHI98PP code.

	Fe	Co	Sb	Tl
Type	H	H	TM	H
Configuration	$4s^1\ 3d^6\ 4p^0$	$4s^1\ 3d^7\ 4p^0$	$5s^2\ 5p^3$	$6s^2\ 5d^{10}\ 6p^0$
Local part	f	f	s	p
s-channel	1.2	1.2	1.8	1.4
p-channel	1.2 (5.0)	1.2 (5.0)	2.0	1.4
d-channel	1.0	1.0	2.5 (15.0)	1.4
f-channel	1.6[a]	1.6[a]	–	1.6[a]
r_{nlc}	0.9	0.9	1.5	1.0

[a]Default value used by the FHI98PP code

B. Electronic properties

The left part of Fig. 1 shows the LDA band structure of $CoSb_3$ between the high symmetry points N, Γ, and P. The top of the valence bands has been fixed at 0 eV. There is a good agreement between our results and the band structures obtained in previous studies[28,29,30,31]. We observe the presence of two well separated groups of valence bands. The bands between -13 eV and -7 eV are mainly composed of Sb 5s states while the valence bands above -6 eV result from hybridizations between Sb 5p and Co 3d bands.

There is some controversy about the energy of the band gap, E_g, in $CoSb_3$. Experimentally, values between 0.03 eV and 0.7 eV have been reported [see Refs. 32,33,34 and references therein]. From a theoretical point of view, there is a similar strong discrepancy between the values in the litterature. The bandgap is defined by a highly dispersive band at the Γ-point. We obtain a value of 0.24 eV in reasonable agreement with other first-principles LDA and GGA calculations [0.05 eV[29], 0.22 eV[28], 0.195 & 0.330 eV[30], 0.140 eV[31]]. This discrepancy between the theoretical results has been attributed to a strong dependence of E_g on the position of the Sb atoms together with the well-known problem of the LDA and GGA to predict the correct bandgap of semiconductors[28,30].

In the $TlFeCo_3Sb_{12}$, [right part of Fig. 1], the bandgap (0.20 eV) is slightly smaller than in the unfilled compound. In addition, we observe two additional groups of bands that are related to the atomic orbitals of Tl. The Tl 5d states form a flat set of bands that are in the same energy region as the Sb 5s states. Due to the lack of dispersion, these states can be considered as inerte. At the opposite, the Tl 6s states form a band about -7 eV that shows a significant dispersion related to a covalent interaction with the electronic states of the host crystal. This point will be investigated in more detail below.

In some cases, the filling of the voids in skutterudites does not only affect the lattice thermal conductivity but also the electronic transport properties. For example, the

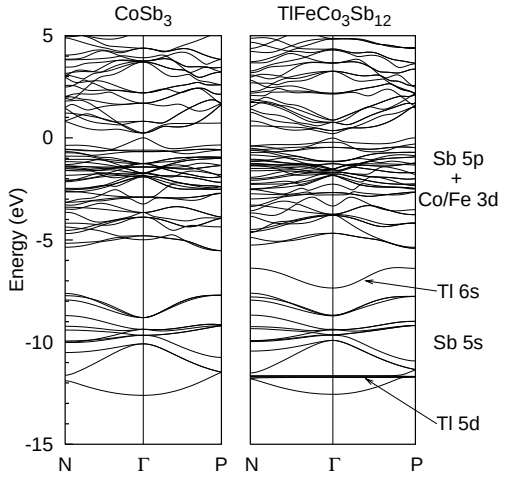

FIG. 1: Electronic band structure in $CoSb_3$ and $TlFeCo_3Sb_{12}$.

Ce 4f states in $CeFe_4Sb_{12}$ hybridize with the Fe 3d and Sb 5p states to form a set of flat conduction bands in the vincinity of the Fermi level[8]. Due to the low dispersion of these bands, the electron effective mass in this compound is quite high implying a low electron mobility[35]. As it can be seen in the right part of Fig. 1, the effect of Tl filling on the electronic band structure of $CoSb_3$ is less important. The only additional bands ly well below the Fermi level and will therefore not affect the electronic transport properties. However, in order to conclude definitively about this point, it might be important to perform a more intensive study of the electronic band structure of $TlFeCo_3Sb_{12}$ that eventually takes into account spin-orbit coupling.

In order to get additional informations on the electronic properties of $CoSb_3$ and $TlFeCo_3Sb_{12}$, we computed the localization tensor (see Ref. 36 and references therein) and the electronic density for selected states in these compounds. As we have shown in a previous

work[22], the decomposition of the localization tensor into contributions of individual groups of bands can act as a sensitive probe to study hybridizations within a solid. For example, a state that has the same variance in a solid and in the isolated atom can be considered as chemically inerte. At the opposite, a modification of the variance is usually attributed to covalent interactions of the corresponding orbitals.

In $CoSb_3$ and $TlFeCo_3Sb_{12}$ the localization tensor is isotropic. In Table II, we report the variances of the two (resp. three) groups of bands defined in Sec. III B as well as the variances of the atomic orbitals Sb 5s, Tl 5d and Tl 6s. In case of Tl, we used linear response calculations to obtain the variance of the 6s state of an isolated Tl^+ ion. We adopted this configuration because it is close to the configuration we expect for Tl in $TlFeCo_3Sb_{12}$. Moreover, it allowed us to avoid some problems related to the linear response calculation of the localization tensor for partially occupied states. To use the same approach for Sb, we had to chose Sb^{3+} as reference configuration. For the 5s state, we obtained a value of 1.51 bohr^2. Unfortunately, the character of the bonding of Sb in $CoSb_3$ is rather covalent than ionic. The Sb^{3+} configuration seems therefore somewhat artificial. To compute the variance for the neutral Sb atom, we used the FHI98PP[14] code to compute the all-electron wavefunction of the 5s state and its variance as a matrix element of the squared position operator x^2.

TABLE II: Variances $\langle r^2 \rangle_c$ (Bohr^2) of the groups of bands in $CoSb_3$ and $TlFeCo_3Sb_{12}$ and of the Sb 5s, Tl 5d and Tl 6s electrons calculated on an isolated Sb atom and Tl^+ ion.

Bands	$CoSb_3$	$TlFeCo_3Sb_{12}$	Atom
Sb 5s (+ Tl 5d)	3.06	2.63	1.86[a], 0.85[b]
Tl 6s	—	18.06	2.14
Sb 5p + Co 3d	5.11	5.85	—
E_g (eV)	0.24	0.20	—

[a] Sb 5s orbital of an isolated Sb atom.
[b] Tl 5d orbitals of an isolated Tl^+ ion.

In $CoSb_3$, the variance of the Sb 5s bands is larger than the variance of the corresponding atomic orbital. This result confirms the participation of these electrons in the Sb-Sb bonding observed previously[30]. In the filled compound, the Tl 5d states occupy the same energy region as the Sb 5s states. Therefore, the formalism of Ref. 22 cannot be applied to study the localization of these bands individually. Nevertheless, we can obtain some information on the modification of the Sb 5s states in $TlFeCo_3Sb_{12}$. Due to the flat dispersion of the Tl 5d bands observed in Fig. 1, it is reasonable to assume that their variance in the solid is close to the value in the isolated Tl^+ ion. If we neglect the covariance between Sb 5s and Tl 5d bands, we obtain a value of 3.37 Bohr^2 for the variance of the Sb 5s bands in $TlFeCo_3Sb_{12}$. This result suggests that the Sb 5s electrons are more delocallized in the filled compound than in the unfilled. It remains true in case the covariance between Sb 5s and Tl 5d bands is not zero since this quantity is necessarily negative.

A stronger variation is found for the variance of the highest occupied bands (Sb 5p + Co 3d). In $TlFeCo_3Sb_{12}$, these electrons are more delocallized than in $CoSb_3$.

The most spectacular evolution undergoes the variance of the Tl 6s state. In the solid, this quantity is about 9 times larger than in the isolated ion. This result suggests a significant interaction between the Tl 6s orbitals and the electronic states of the host crystal. To get more informations about these hybridizations we show in Figure 2 the electronic pseudo-density associated to the Tl 6s band. As can be seen, these electrons are partially delocallized on the Sb atoms of the cage. This result suggests that there is a significant covalent interaction between Tl and Sb due to the Tl 6s electrons. Such an interaction would be coherent with the fact that Tl can be inserted into the voids of the host crystal in spite of the fact that its ionic radius (1.84 Å) is larger than that of the rare-earth fillers Ce (1.28 Å) and La (1.50 Å) and that it is close to the radius of the cage (about 1.892 Å[37]).

In order to obtain further insight on the electronic properties of skutterudites and the effect of different filling atoms on the band structure it might be interesting to build generalized Wannier functions[38,39] for these compounds.

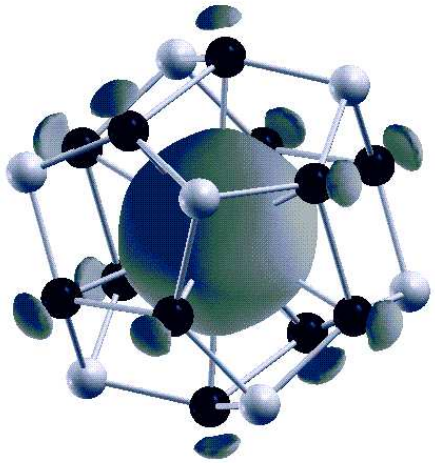

FIG. 2: Electronic pseudo-density of the Tl 6s band in $TlFeCo_3Sb_{12}$. The isodensity value corresponds to 10 % of the maximum density of this state (0.0013 electron/bohr^3). Tl (not shown) occupies the center of the cage. The black and grey spheres represent respectively Sb and Co/Fe. This figure has been realized thanks to the XCrySDen[40] crystalline and molecular structure visualisation program.

In summary, the main differences between the elec-

tronic band structures of $CoSb_3$ and $TlFeCo_3Sb_{12}$ affect the region well below the Fermi level. On the one hand, the Tl 5d states show a flat dispersion suggesting that these states are chemically inerte. On the other hand, the Tl 6s states show a significant dispersion related to a partial delocalization of the corresponding electrons on the Sb atoms of the cage. These hybridizations are expected to affect the dielectric and dynamic properties of Tl in the filled compound.

IV. DIELECTRIC PROPERTIES

A. Optical dielectric tensor

In $CoSb_3$, the dielectric tensor is isotropic. The theoretical value $\varepsilon_\infty = 31.67$ overestimates the experimental result[41] of 25.6 by about 20 % as it is typical in LDA calculations[42]. Similar large dielectric constants as in $CoSb_3$ have been computed for other narrow bandgap semiconductors such as Al_2Ru [principal values: 18.9, 22.9, 20.7][43]. Moreover, they have been measured in a series of skutterudites such as $CoAs_3$ (26.25)[44], UFe_4P_{12} (17) or $CeFe_4P_{12}$ (31)[45].

In the filled compound, the dielectric tensor is no more isotropic but has weak off-diagonal elements. These elements are about four orders of magnitude smaller than the diagonal ones and we will not consider them in the discussion that follows. We obtain a value of 38.57 for the dielectric constant in $TlFeCo_3Sb_{12}$ that is significantly larger than in unfilled $CoSb_3$. Unfortunatley, we are not aware of any experimental data to which we can compare this result. In spite of the error on its absolute value, we expect the evolution of the dielectric constant to be correctly reproduced by our calculation since it is reasonable to assume that the LDA error on ε_∞ is of the same magnitude in both compounds.

The increase of ε_∞ can have distinct origins. On the one hand, based on a simple Clausius-Mossotti model[46], the polarizabilities of the Tl^+ ions add to the dielectric susceptibility of the unfilled compound to yield a larger ε_∞ in $TlFeCo_3Sb_{12}$. On the other hand, the increase can be due to the dielectric constant of the host crystal that is increased due to the presence of Tl and Fe in the filled compound. To check which mechanism applies in $CoSb_3$, we decomposed the optical dielectric tensor into contributions originating from the individual groups of bands of Fig. 1. This decomposition reveals that the deeper bands (Sb 5s, Tl 5d and Tl 6s) are only weakly polarizable by an electric field and contribute less than than 0.1 % to ε_∞ and that the contribution of the Sb 5p and transition metal 3d electrons is strongly increased in the filled compound. We therefore propose that the observed increase of ε_∞ is due to a modification of the dielectric constant of the host crystal while the polarizability of Tl^+ plays only a minor role.

B. Effective ionic charges

In Table III, we report the static ionic charges Q_i in $CoSb_3$ and $TlFeCo_3Sb_{12}$ obtained from a topological analysis following Bader's prescription for the partitioning of space into atomic bassins[17]. In this approach, one has to determine surfaces that obey the zero-flux condition for the electron density $n(\mathbf{r})$: $\boldsymbol{\nabla} n \cdot \boldsymbol{N} = 0$ where $\boldsymbol{N}$ is the vector normal to the surfaces. The integration of $n(\mathbf{r})$ within the atomic bassins yields the ionic charge Q_i of each topological atom i.

In both compounds the chemical bonds have a negligible ionic character as it is revealed by the small Q_i. At the opposite, to these small static charges, the dynamical Born effective charges Z^* (Table IV) are very large, comparable to the giant effective charges in ferroelectric ABO_3 compounds [47] and other narrow bandgap semiconductors such as Al_2Ru[43]. In the ferroelectrics, the amplitude of the Z^* can be explained thanks to the Harrison model[48]. A relative displacement of the B and O atoms generates a giant dipole moment due to a dynamical change of hybridization between O 2p and B d atomic orbitals[49]. In $CoSb_3$, the highest valence bands are basically due to hybridizations between Co 3d and Sb 5p atomic orbitals[30]. Moreover, the structure of this compound is formed of distorted $CoSb_6$ octahedra similar to the BO_6 octahedra of the ABO_3 ferroelectrics. It seems therefore plausible to assume that a similar mechnisme takes place in $CoSb_3$ and that the large effective charges are generated by dynamic changes of hybridizations between Co 3d and Sb 5p atomic orbitals.

In skutterudites, giant effective charges have been measured from infrared spectroscopie for UFe_4P_{12} ($|Z^*_{Fe}| = 8.9$) and $CeFe_4P_{12}$ ($|Z^*_{Fe}| = 11$)[45]. In $CoSb_3$, we obtain[50] a value of 6.04 for $|Z^*_{Co}|$ from the amplitude of the LO-TO splitting reported in Ref. 51 and the optical dielectric constant of Ref. 41. This value is in good agreement with the results reported in Tab. IV.

TABLE III: Bader ionic charges Q_i ($|e^-|$) in $CoSb_3$ and $TlFeCo_3Sb_{12}$.

$CoSb_3$		$TlFeCo_3Sb_{12}$	
		Tl	0.29
Co_1	-0.53	Fe	-0.36
Co_2	-0.53	Co_2	-0.48
Sb	0.17	Sb	0.12

The effective charge of the filling Tl atom is also highly anomalous. It is significantly larger than its static ionic charge reported in Table III. Moreover, it is larger than its nominal ionic charge of +1 that would be expected if there was a complete transfer of the 6p electron to the atoms of the cage. Giant effective charges have been reported previously[45] for the filling atoms U and Ce in FeP_4. Their values of $Z^*_U = 8.9$ and $Z^*_{Ce} = 8.7$ are even larger than the value of Z^*_{Tl} in $CoSb_3$.

The effective charges of Co and Sb are similar in the

TABLE IV: Born effective charges ($|e^-|$) in $CoSb_3$ and $TlFeCo_3Sb_{12}$.

$CoSb_3$				$TlFeCo_3Sb_{12}$			
				Tl	3.64	-0.05	-0.02
					-0.02	3.64	-0.05
					-0.05	-0.02	3.64
Co_1	-6.89	0.82	0.34	Fe	-9.83	1.13	-0.20
	0.34	-6.89	0.82		-0.20	-9.83	1.13
	0.82	0.34	-6.89		1.13	-0.20	-9.83
Co_2	-6.89	-0.82	-0.34	Co_2	-7.28	-0.75	0.08
	-0.34	-6.89	0.82		-0.09	-7.30	0.73
	-0.82	0.34	-6.89		-0.64	-0.10	-7.34
Sb	2.63	0.00	0.42	Sb	2.43	-0.10	-0.04
	0.00	1.94	0.00		-0.03	1.87	0.01
	0.68	0.00	2.32		1.01	0.12	2.13

filled and the unfilled compound. The excess effective charge introduced by Tl can therefore not be compensated by these two atoms in order to satisfy the charge neutrality condition[20] $\sum_\kappa Z^*_{\kappa,\alpha\beta} = 0$. As can be seen in Table IV, $|Z^*_{Fe}|$ is about $3|e^-|$ larger than the absolute value of the effective charge of the Co atom that it substitutes. As mentioned in Sec. III A, the 6p electron of Tl is compensated by a hole in the 3d orbitals of Fe. In case of the Born effective charges, Fe plays a similar role: due to the fact that $|Z^*_{Fe}|$ is larger than $|Z^*_{Co}|$, the anomalous effective charge of Tl is mainly compensated by the anomalous effective charge of Fe. A plausible mechanism for this compensation could be that the Tl 6p electron is partially shared between Tl and Fe so that it might be responsible for a transfer of charge during a relative displacement of these two atoms.

V. ZONE-CENTER PHONONS

A. Potential energy

To understand the effect of Tl-filling on the lattice thermal conductivity of $CoSb_3$, it is mandatory to investigate the dynamics of these atoms in their cages. Experimentally, unusually large atomic displacement parameters (ADP's) have been observed for various filling atoms[3,35]. To decide whether these ADP's are due to quasi-harmonic vibrations about the center of the cage or to the random hopping between off-center sites[37], it is important to investigate the shape of the potential energy well.

To determine the shape of the Tl potential, we computed the variations of the total energy for atomic displacements along various directions. Figure 3 shows the results for the cristallographic direction [1 0 0]. We see that the center of the cage is the global minimum of the potential energy well and not a saddle point as it has been suggested previously[37]. Close to the origin, the energy changes quadratically with the atomic positons [dashed line]. The whole energy region of Fig. 3 can be fit accurately by a polynome of degree six [full line]. The harmonic frequency is 52 cm^{-1}. This so-called "bare frequency" is quite independent of the direction of the atomic displacement. For the directions [1 1 0] and [1 1 1], we obtaiend values that differ by less than 0.3 cm^{-1} from the one of Fig. 3. In case of Tl, the bare frequency is smaller than the one of Ce (68 cm^{-1}) and La (74 cm^{-1}) in $FeSb_4$[6]. This difference is attributed to the larger mass of Tl and to the curvature of the potential energy at the origin that is significantly smaller in case of Tl (2.0371 eV/Å) than for Ce (2.3943 eV/Å) and La (2.8005 eV/Å). This result is surprising. On the basis of the crystal radii[52] of Tl^{1+} (1.84 Å), Ce^{4+} (1.28 Å) and La^{3+} (1.50 Å) in a 12-coordinate site we could expect the repulsion betwenn ionic cores to be more important between Tl and Sb than between Ce/La and Sb. The eneregy should therefore increase more rapidly for an off-center displacement of Tl and the curvature of the potential energy well should be stronger. However, in Sec. III B we saw that there is a significant covalent interaction between Tl and Sb. The simple argument of the crystal radii can therefore not be applied in case of $TlFeCo_3Sb_{12}$ because the atoms do not behave like rigid spheres.

The large ADP's of Tl have been attributed to an Einstein oscillator[3] with a characteristic frequency of 36 cm^{-1}. This value is close to the Einstein frequencies deduced from specific heat measurements and inelastic neutron scattering experiments[9] (39 ± 1 cm^{-1}) but it is significantly lower than the computed Tl bare frequency. This difference between the bare frequency and the normal mode frequency observed experimentally will be further discussed in Sec. V B.

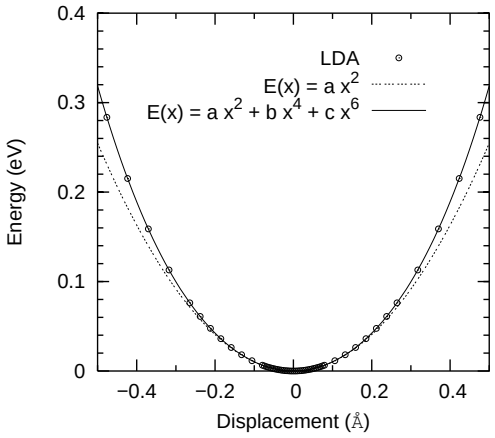

FIG. 3: Potential energy associated to a cooperative displacement of Tl along [1 0 0].

B. Normal mode frequencies

The unfilled skutterudite $CoSb_3$ belongs to the space group $Im\overline{3}$. At the Γ-point, the zone center optical phonons can be classified according to its irreductible representations into

$$2A_g + 2E_g + 4F_g + 2A_u + 2E_u + 7F_u. \qquad (1)$$

Only the F_u-modes are infrared active. At the Γ-point, they are split into transverse (TO) and longitudinal (LO) modes. The A_g, E_g and F_g are Raman active.

In Table V, we report the frequencies (cm^{-1}) of the TO and LO modes in $CoSb_3$ and $TlFeCo_3Sb_{12}$. The values in the unfilled compound are compared to the first-principles and force-constant (FC) model calculations of Feldman and Singh [model A of Ref. 26] and to the experimental data obtained by infrared[51] and Raman[53] spectroscopy. The overall agreement between theory and experiment is quite good. Especially the phonon frequencies in the low energy region — the region of the Tl vibrations in the filled compound — are accurately reproduced by our first-principles calculations.

We should note that the Raman measurements of Ref. 53 were performed on polycrystalline samples. As a consequence, only the A_g modes were identified in this study while the remaining Raman lines can be either associated to E_g or F_g modes. In Table V, we identify four of the additional frequencies to the theoretical F_g modes. In fact, the experimental frequencies of 82, 109 and 152 cm^{-1} are close to the three lowest F_g modes obtained in our study and by Feldman and Singh[26]. In case of the mode at 178 cm^{-1}, this identification is less clear since its frequency is close to the highest E_g mode and the highest F_g mode. In addition to these four modes, the authors of Ref. 53 report a mode at 60 cm^{-1} [not reported in Table V] that is not confirmed by our calculation neither by the calculation of Feldman and Singh [26]. Therefore, we do not associate this Raman line to a phonon mode in $CoSb_3$.

In spite of the giant effective charges, the transverse and longitudinal F_u modes are rather close in energy. This small amplitude of the LO-TO splitting can be attributed to the large optical dielectric constant (see Sec. IV A) that effectively screens the macroscopic electric field generated by the longitudinal polar lattice vibrations. At lower energies, this screening is almost perfect and the LO and TO modes are nearly degenerated. At higher energies, we observe a small increase in the frequency of the LO modes with respect to the TO modes. We will see in the next section that the low and high energy regions are respectively dominated by vibrations of Sb and Co. The larger amplitude of the LO-TO splitting at higher energies can therefore be attributed to the giant effective charges of Co that are about three times larger than those of Sb.

In the filled compound $TlFeCo_3Sb_{12}$, the presence of Fe breaks the symmetry of the crystal lattice. As a consequence, it is no more possible to classify the phonon modes according to Eq. (1). Nevertheless, the eigenvectors of most phonons are only slightly modified in the filled compound. By computing their overlap, it is therefore possible to associate each phonon in $TlFeCo_3Sb_{12}$ to a mode in the unfilled compound. Due to the symmetry breaking, the degeneracy of some phonons is left in $TlFeCo_3Sb_{12}$. In this case, we report the frequencies of all the resulting modes if they differ by more than one cm^{-1}. The first and second values in the last column of Table V are respectively one and two times degenerated.

The TO modes that have the strongest overlap with the F_u^T modes of the unfilled compound, are polar. The single and double degenerate modes are respectively polarized in the [1 1 1] direction and in the plane perpendicular to [1 1 1]. The frequencies of the corresponding LO modes are reported at the end of Tab. V. In addition to the F_u modes other modes become polar in the filled compound. Among them, the highest A_u and E_u modes acquire the strongest polarity. Nevertheless, the splitting between the corresponding TO and LO modes is rather weak and not reported in Table V.

At 40 cm^{-1}, we observe three additional polar modes that are absent in the unfilled compound. Experimentally, a peak in the phonon density of states of $TlFeCo_3Sb_{12}$ has been observed at this frequency[9]. This peak has been attributed to a locallized vibration of Tl in his cage. Our calculation confirms the strong contribution of Tl to these modes. About 88 % of the eigenvectors are due to the vibrations of Tl. The frequencies of these modes are significantly smaller than the bare frequency of a pure (100 %) Tl vibration reported in Sec. V A (52 cm^{-1}). This difference between the bare frequency and the frequency of the local Tl mode (LM) can be attributed to hybridizations between the pure Tl vibrations and the phonons of the unfilled compound.

To the authors knowledge, no experimental data on the zone-center phonons of $TlFeCo_3Sb_{12}$ are available. However, in a recent work, Feldman and co-workers[7] measured the frequencies of the Raman active modes in $La_{0.75}Fe_3CoSb_{12}$. In addition, they used first-principles calculations to compute the frequencies of all zone-center optical phonons in $LaFe_4Sb_{12}$. The results of teir studies are reported in Table V where they are compared to our theoretical results for $TlFeCo_3Sb_{12}$ although they have been obtained for a different compound. However, the Raman active modes are dominated by the dynamics of Sb. In Sec. VI, we will see that the vibrations of Sb are almost decoupled of Co/Fe. We can therefore expect the frequencies of the Raman active modes to be similar in $TlFeCo_3Sb_{12}$ and the La-filled skutterudites. In Table V, we see that this is indeed the case and that the agreement between our results and those of Feldman and co-workers is quite good for most of the Sb-dominated modes between 80 and 200 cm^{-1}. The frequency of the La-dominated mode in $LaFe_4Sb_{12}$ is larger than that of the Tl-dominated mode in $TlFeCo_3Sb_{12}$. This result will be discussed more in detail in Sec. VI.

TABLE V: Frequencies (cm^{-1}) of the transverse and longitudinal zone-center optical phonons in $CoSb_3$ and $TlFeCo_3Sb_{12}$. The phonons in the unfilled compound are classified according to the irreductible representations of the space groupe $Im\bar{3}$. Each phonon in $TlFeCo_3Sb_{12}$ is associated to the mode of the unfilled compound for which the overlap between eigenvectors is the strongest. In case the degeneracy of a mode is left in the filled compound, we report the frequencies of all resulting phonons. The first and second values in column 6 are respectively one and two times degenerated. The values of Ref. 7 in the two last columns have been obtained for La-filled $FeSb_3$ for which the lattice dynamics is expected to be similar to that in $CoSb_3$.

Mode	Unfilled				Filled		
	LDA[a]	LDA[b]	FC[b]	Exp.	LDA[a]	LDA[f]	Exp.
LM^T					41, 42	54	40[e]
LM^L					45		
A_g	141	150	151	135[c]	145	148	147[f]
	169	179	177	186[c]	155	156	154[f]
A_u	116	109	110		112	92	
	236	241	240		224	212	
E_g	122		139		123	133	122[f]
	175		183		157	158	161[f]
E_u	133		131		130	125	
	246		267		228	251	
F_g	87		83	82[c]	93, 92	95	94[f]
	105		97	109[c]	98,101	101	102[f]
	143		157	152[c]	133,136	137	131[f]
	173		178	178[c]	166,163	164	172[f]
F_u^T	80		78	78[d]	85	94	
	117		120	120[d]	116	119	
	136		144	144[d]	137,135	140	
	167		175	174[d]	152	151	
	232		241	247[d]	217,215	223	
	245		261	257[d]	248,233	241	
	258		277	275[d]	238,261	259	
F_u^L	80			81[d]	85		
	119			124[d]	118		
	137			147[d]	137,135		
	168				152		
	244			252[d]	233,230		
	250			262[d]	244,241		
	273			288[d]	267,274		

[a]Present: $CoSb_3$ and $TlFeCo_3Sb_{12}$
[b]LDA and force-constnat (FC) model calculations[26] for $CoSb_3$
[c]Raman spectroscopy[53] for $CoSb_3$
[d]Infrared spectroscopy[51] for $CoSb_3$
[e]Inelastic neutron scattering[9] for Tl-filled $CoSb_3$
[f]LDA + Raman data on La-filled $FeSb_3$[7]

C. Infrared reflectivity and static dielectric tensor

The static dielectric constant ε_0 can be decomposed into an electronic and an ionic part[54]

$$\varepsilon_0 = \varepsilon_\infty + \sum_m \Delta\varepsilon_m. \quad (2)$$

$\Delta\varepsilon_m$ represents the contribution of an individual zone-center TO mode and can be computed from the infrared oscillator strenght S_m, the phonon frequency ω_m and the unit cell volume Ω_0

$$\Delta\varepsilon_m = \frac{4\pi}{\Omega_0}\frac{S_m}{\omega_m^2}. \quad (3)$$

In Table VI, we report the decomposition of ε_0 in $CoSb_3$ and $TlFeCo_3Sb_{12}$. In the unfilled compound, the ionic contribution is dominated by the F_u mode at 232 cm^{-1} that has the strongest oscillator strength ($S_m = 14.29 \cdot 10^{-4} a.u.$). Such a large value can be compared to the oscillator strenghts of the high polar modes in ferroelectric oxides such as $LiNbO_3$[55]. In addition, the frequency of this mode is of the same magnitude as the frequency of the most polar modes in $LiNbO_3$. However, the $\Delta\varepsilon_m$ is small compared to the ionic contribution to ε_0 in the ferroelectrics. This surprising result is due to the fact that $CoSb_3$ has a relatively open structure characterized by a large unit cell volume. In $CoSb_3$, the primitive unit cell contains 16 atoms and has a volume $\Omega_0 = 369.20 \mathring{A}^3$ that is more than three times larger than the volume of the 10 atom unit cell in $LiNbO_3$ ($\Omega_0 = 101.70 \mathring{A}^3$).

TABLE VI: Electronic and ionic contributions of individual phonon modes to the static dielectric constant in $CoSb_3$ and $TlFeCo_3Sb_{12}$.

	$CoSb_3$		$TlFeCo_3Sb_{12}$	
	ω_m (cm^{-1})	$\Delta\varepsilon_m$	ω_m (cm^{-1})	$\Delta\varepsilon_m$
Electronic		31.67		38.57
LM			41, 42	10.77
F_u	80	0.09	85	0.07
A_u			112	0.00
F_u	117	1.76	116	2.00
E_u			130	0.02
F_u	136	0.38	137,135	0.23
F_u	167	0.09	152	0.13
F_u	232	6.44	217,215	8.04
A_u			224	0.93
E_u			228	0.06
F_u	245	0.49	248,233	0.94
F_u	258	1.52	238,261	2.07
Total		42.44		63.83

In $TlFeCo_3Sb_{12}$, the static dielectric tensor is no more isotropic but presents weak off-diagonal elements. As for the optical dielectric tensor, these elements are about two orders of magnitude smaller than the diagonal ones. To a good approximation, we can therefore neglect them and characterize the dielectric tensor by its single diagonal element ε_0. The decomposition of ε_0 in the filled compound is more complicated than in the unfilled. The values reported for the F_u modes in Tab. VI correspond to the sum of the $\Delta\varepsilon_m$ of the three modes that have been splitted in the filled compound (see Sec. V B).

In $TlFeCo_3Sb_{12}$, ε_0 is about 50 % larger than in unfilled $CoSb_3$. Part of this evolution can be attributed

to the electronic contribution that increases by 6.89 as discussed in Sec. IV A and to the ionic contribution of the F_u modes that is slightly larger in the filled compound. In addition, due to its lower symmetry, the A_u and F_u modes become infrared active in the filled compound although theyr contribution to ε_0 is quite weak. The most important part (10.77) comes from the Tl dominated mode at 42 cm^{-1}. It's oscillator strength ($S_m = 0.79 \cdot 10^{-4} a.u.$) is rather low compared to that of the Co/Fe dominated modes at high energy. But due to its low frequency, the constribution of this additional mode in the filled compound is very important. This result demonstrates that Tl-filling has an important influence on the static dielectric constant of $CoSb_3$. It suggests that materials with a structure characterized by large empty voids might be interesting candidates for applications that require a well defined dielectric constant since the value of ε_0 can be tuned by filling the voids (or a fraction of voids) with foreign atoms.

From the analysis of the results presented in this paper, we can identify some general criteria that should be satisfied by an element in order to be efficient for such a tuning of the dielectric constant. First, the Born effective charge of the filling atom should be as high as possible. This requires a certain amount of hybridizations between the foreign atoms and the atoms of the host crystal. Second, the bare frequency of the filling atom should be as low as possible since we expect the normal mode frequency to increase with the bare frequency. On the one hand, this criterion requires that, in spite of the hybridizations necessary for a high polarizability and Born effective charge, the filling atom should only be weakly bound to ensure a low curvature of the potential energy well. On the other hand, the mass of the filling atom M should be high since the bare frequency is proportional to $1/\sqrt{M}$.

Fig. 4 shows the infrared reflectivity of $CoSb_3$ (a) and $TlFeCo_3Sb_{12}$ (b) computed from the Born effective charges and phonon frequencies and eigenvectors as it is described in Ref. 54. Since this approach neglects the damping of the phonon modes, the curves saturate to 1. For the unfilled compound, there is a qualitative good agreement between Fig. 4 (a) and the reflectivity measured by Lutz and Kliche[41,51]. The most striking difference between the reflectivity of $CoSb_3$ and $TlFeCo_3Sb_{12}$ is the presence of a well defined band below 50 cm^{-1} that is related to the Tl-dominated mode and the large Tl Born effective charge (Sec. IV B). In addition, we observe the appearance of a few lines associated to the A_u and E_u modes that become infrared active in the filled compound as discussed above. Unfortunately, we are not aware of any experimental reflectivity measurements for $TlFeCo_3Sb_{12}$. However, Dordevic and co-workers[45] measured the reflectivity of MFe_4P_{12} filled skutterudites (M = La, Th, Ce, U). They observed a similar strong band associated to the M-dominated mode in these compounds. This shows that infrared spectroscopy is an appropriate technique to study the dynamics of the filling atoms in skutterudites.

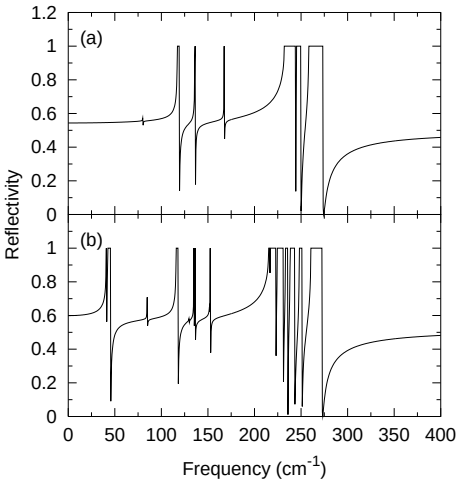

FIG. 4: Infrared reflectivity of $CoSb_3$ (a) and $TlFeCo_3Sb_{12}$ (b).

VI. PHONON DISPERSION CURVES, DENSITY OF STATES AND SPECIFIC HEAT

Fig. 5 shows the phonon dispersion relation and projected DOS of $CoSb_3$ (a) and $TlFeCo_3Sb_{12}$ (b). In both compounds, the vibrations of Co/Fe and Sb are mainly decoupled and occupy respectively the high energy region above 220 cm^{-1} and the low energy region below 200 cm^{-1}.

The computed DOS of $CoSb_3$ is in good agreement with the DOS obtained from various force constant model calculations by Feldman and Singh[26]. At low frequency, the agreement is nearly perfect. All calculations also predict a large gap at about 200 cm^{-1} and a smaller gap at about 100 cm^{-1}. We do not properly reproduce the two well defined peaks above 200 cm^{-1} reported in Ref. 26 (calculations) and Ref. 56 (experiment). This might be due to a lack of accuracy in our calculation of the high energy part of the spectrum. In Tab. V, we see that the frequencies above 200 cm^{-1} tend to underestimate the experiment while those below 200 cm^{-1} are more accurate. The small deviations at high energy do not affect the following discussions that focus on the lower part of the spectrum.

In the filled compound, an additional branch at about 40 cm^{-1} gives rise to a well defined peak in the DOS that is not present in the unfilled compound. A peak at the same frequency has been observed by inelastic neutron scattering[9] in the DOS of Tl-filled $CoSb_3$. By comparing the DOS of the filled and unfilled compound, the authors of Ref. 9 attributed this peak to a locallized oscillation of Tl. As can be seen in Fig. 5, the peak at 40 cm^{-1} is strongly dominated by the vibrations of Tl that show only weak hybridizations with Sb. This result gives therefore a strong argument in favour of the interpretation of Ref. 9.

Experimentally, a difference has been observed between the DOS of Tl- and La-filled skutterudites. The authors of Ref. 9 report the existence of a single Tl-dominated peak in $TlFeCo_3Sb_{12}$ at 40 cm^{-1} while the authos of Ref. 5 claim that there are two La-dominated peaks in the DOS of $LaFe_4Sb_{12}$ at 56 and 121 cm^{-1}. Our calculation clearly confirms the existence of a single peak in $TlFeCo_3Sb_{12}$ (solid line in Fig. 6). In Sec. V A, we saw that the bare frequency of Tl (52 cm^{-1}) is significantly smaller than that of La (74 cm^{-1}), a difference that must be attributed to the larger Tl mass and a weaker curvature of the Tl potential energy well. If we redo the calculations for a fictitious compound in which we artificially reduce the mass of Tl to that of La, the Tl vibrational frequency is shifted to 48 cm^{-1} and yields a marginal increase in the DOS around 100 cm^{-1} (dashed line in Fig. 6). Further, if we artificially strengthen the interaction of Tl with the lattice by increasing the interatomic force constants in order to fit the curvature of the potential energy well of La, the main Tl vibrational peak is shifted at 51 cm^{-1} whereas we observe the appearance of a second peak around 100 cm^{-1}. This strongly suggests that the peak at 121 cm^{-1} reported by Keppens and co-workers[5] cannot be attributed to an additional localized mode but rather to phonon modes that are formed by coupled Sb-La vibrations. Generally, it appears that the coupling between the La and Sb vibrations is more important than between those of Tl and Sb because in the former case, the bare frequency is closer to the energy region of the Sb-dominated optical phonons. This interpretation of the second peak is consistent with the one drawn by Feldman and co-workers in Ref. 6.

As discussed above, the vibrations of Co/Fe are located in the high energy region of the phonon spectrum so that they are mainly decoupled from the vibrations of Tl. This result allows us to justify the approximation used in our study to negelect any disorder due to the random substitution of one Co atom per cell by Fe (see Sec. II). Since the vibrations of Tl and Co/Fe are only weakly coupled, we expect the influence of the disorder on the lattice dynamics of Tl to be small. This hypothesis is further confirmed by the observation that the Tl-peak in the experimental DOS[9] is broader in the Sn compensated compound $TlCo_4Sb_{11}Sn$ than in $TlFeCo_3Sb_{12}$. In fact, the vibrations of Tl are located in the same energy region as that of Sb/Sn. As a consequence, there are significant hybridizations between the vibrations of those atoms. We expect therefore that the disorder due to the random substitution of one Sb per cell by Sn has a stronger influence on the dynamics of the filling atom than that of Co by Fe.

Due to the rather flat dispersion of the optical branches, we expect the lattice termal conductivity of $CoSb_3$ to be dominated by the acoustic phonons. As can be seen in Fig. 5 (b), the Tl-derived modes cut through the acoustical branches. A similar effect has been observed recently in Sr-filled Ge clathrates from atomic simulations making use of empirical interatomic potentials[57]. Using molecular dynamics simulations, the authors of Ref. 57 showed that the Sr derived modes reduce the lattice thermal conductivity of the clathrates by approximately one order of magnitude by scattering the heat-carrying acoustical phonons. This scattering is enhanced at the frequency of the Sr-modes because of the resonant interaction with the acoustical phonons[58,59,60]. It is therefore reasonable to assume that the resonant interaction between the Tl-derived modes and the acoustical branches has a similar strong effect on the thermal conductivity of $CoSb_3$ and that it is one major source of the important decrease observed experimentally[3].

Fig. 7 shows the heat capacity at constant volume of $CoSb_3$ and $TlFeCo_3Sb_{12}$ computed by integrating the phonon DOS as described in Ref. 25. Our results are compared to the experimental values of Ref. 9 measured for $CoSb_3$ and $Tl_{0.8}Co_4Sb_{11}Sn$ at constant pressure. For the unfilled compound, the agreement between theory and experiment is excellent. In the filled compound, we observe a slight deviation from the experimental data. Part of the discrepancy can probably be attributed to the fact that the experiment has been performed on a Sn-compensated sample with only partial void-filling. Especially the substitution of Sb by Sn is likely to have a stronger effect on the specific heat at low temperatures than the substitution of Co by Fe since the Sb/Sn vibrations are at lower energy than that of Co/Fe.

VII. CONCLUSIONS

In this work, we used first-principles DFT calculations to study the electronic, dielectric and dynamical properties of $CoSb_3$ and $TlFeCo_3Sb_{12}$.

Because of hybridizations between Tl and Sb, the Tl 6s electrons are partially delocalized on the Sb atoms. This result is consistent with the fact that Tl can be inserted into the voids of $CoSb_3$ inspite of its rather large ionic radius.

The electronic dielectric constant of $CoSb_3$ and $TlFeCo_3Sb_{12}$ are quite large with a significantly larger value in the filled compound. This increase cannot be explained in the framework of a Clausius-Mossotti model where the Tl^+ polarizability is supposed to add to the dielectric constant of $CoSb_3$. Instead, it is the dielectric constant of the host crystal itself that is increased upon Tl-filling accompagnied by a substitution of one Co atom per cell by Fe.

Due to the negligible ionic character of the chemical bonds in $CoSb_3$ and $TlFeCo_3Sb_{12}$, the *static* atomic charges of both compounds are rather small. In contrast, the *dynamic* Born effective charges are found to be very large and of the same amplitude as in ferroelectric oxides.

The computation of the energy as a function of a cooperative displacement of Tl revealed that the center of the cage is the global minimum of the potential energy and not a saddle point as it has been suggested previously. In the filled compound, the presence of Tl gives

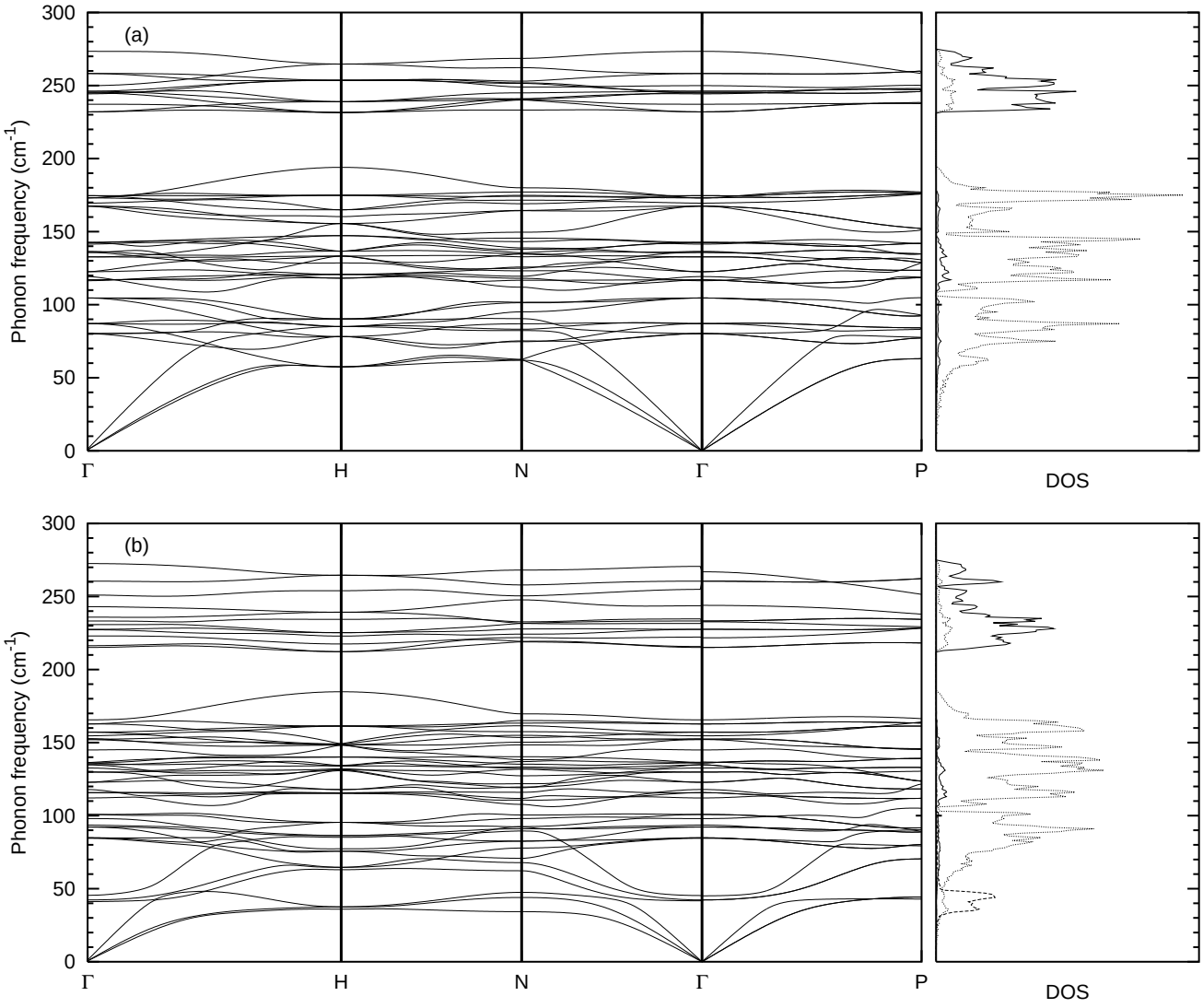

FIG. 5: Phonon dispersion and projected DOS in $CoSb_3$ (a) and $TlFeCo_3Sb_{12}$ (b). The full, dashed and dotted lines in the DOS show respectively Co/Fe, Tl and Sb vibrations.

rise to a *single* peak in the phonon DOS. Due to the hybridizations between the vibrations of Tl and Sb, this peak is significantly lower in frequency than the Tl bare frequency computed from the curvature of the potential energy well. However, these hybridizations are modest compared to those of the La-filled skutterudites where they give rise to a second La peak in the DOS.

The Tl dominated mode at the Γ-point is polar and gives rise to a well defined band in the infrared reflectivity spectrum at low frequency and a strong increase of the static dielectric constant in the filled compound. On the one hand, this result shows that infrared spectroscopy can act as a sensitive probe to study the lattice dynamics of the filling atom in skutterudites and related compounds such as clathrates. On the other hand, it suggests that the dielectric constant of materials characterized by an open structure containing empty voids can be tuned by filling the voids with foreign atoms.

VIII. ACKNOWLEDGMENTS

The authors are grateful to R. P. Hermann, F. Grandjean, G. J. Long and J. P. Issi for helpful discussions. M. V. acknowledges financial support from the FNRS Belgium. This work was supported by the Volkswagen-Stiftung within the project "Nano-sized ferroelectric Hybrids" (I/77 737), the Region Wallonne (Nomade, project 115012), FNRS-Belgium through grants 9.4539.00 and 2.4562.03, and the European Commission through the FAME Network of Excellence (Functional Advanced Materials Engineering of Hybrids and Ceramics).

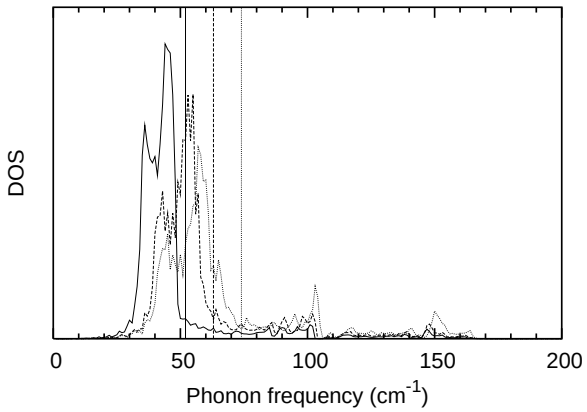

FIG. 6: Tl projected DOS in $TlFeCo_3Sb_{12}$ (full line), Tl projected DOS where we artificially decreased the mass of Tl to that of La (dashed line) and Tl projected DOS where we changed both the mass and the curvature of the potential energy well to those of La (dotted line). The vertical lines indicate the position of the corresponding bare frequencies.

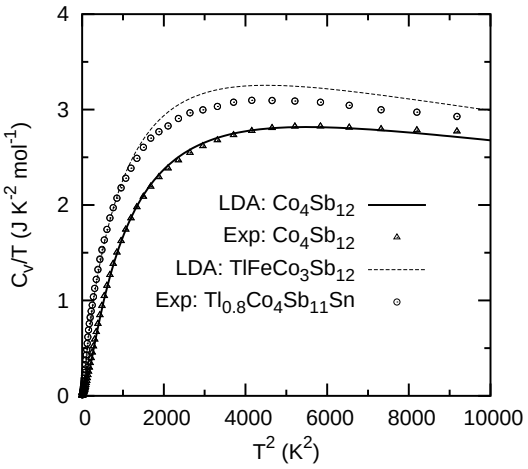

FIG. 7: Theoretical and experimental heat capacity of $CoSb_3$ and Tl-filled $CoSb_3$ divided by the temperature as a function of the square of the temperature. Experimental results are from Ref. 9.

[1] C. Uher, Semiconductors and semimetals **69**, 139 (2001).
[2] B. C. Sales, D. Mandrus and R. K. Williams, Science **272**, 1325 (1996).
[3] B. C. Sales, B. C. Chakoumakos and D. Mandrus, Phys. Rev. B **61**, 2475 (2000).
[4] C. Wood, Rep. Prog. Phys. **51**, 459 (1988).
[5] V. Keppens, D. Mandrus, B. C. Sales, B. C. Chakoumakos, P. Dai, R. Coldea, M. B. Maple, D. A. Gajewski, E. J. Freeman and S. Bennington, Nature **395**, 876 (1998).
[6] J. L. Feldman, D. J. Singh, I. I. Mazin, D. Mandrus and B. C. Sales, Phys. Rev. B **61**, R9209 (2000).
[7] J. L. Feldman, D. J. Singh, C. Kendziora, D. Mandrus and B. C. Sales, Phys. Rev. B **68**, 94301 (2003).
[8] L. Nordström and D. J. Singh, Phys. Rev B **53**, 1103 (1996).
[9] R. P. Hermann, R. Jin, W. Schweika, F. Grandjean, D. Mandrus, B. C. Sales and G. J. Long, Phys. Rev. Lett. **90**, 135505 (2003).
[10] P. Hohenberg et W. Kohn, Phys. Rev. **136**, B864 (1964).
[11] W. Kohn et L. J. Sham, Phys. Rev. **140**, A1133 (1965).

[12] X. Gonze, J.-M. Beuken, R. Caracas, F. Detraux, M. Fuchs, G.-M. Rignanese, L. Sindic, M. Verstraete, G. Zerah, F. Jollet, M. Torrent, A. Roy, M. Mikami, Ph. Ghosez, J.-Y. Raty and D.C. Allan, Computational Materials Science **25**, 478 (2002); [URL www.abinit.org].

[13] J. P. Perdew and Y. Wang, Phys. Rev. B **45**, 13244 (1992).

[14] M. Fuchs and M. Scheffler, Comuter Physics Communications **119**, 67 (1999).

[15] N. Troullier and J. L. Martins, Phys. Rev. B **43**, 1993 (1991).

[16] D. R. Hamann, Phys. Rev. B **40**, 2980 (1989).

[17] R. F. W. Bader, *Atoms in Molecules: A Quantum Theory* (Oxford University Press, Oxford, 1990).

[18] P. Casek, S. Bouette-Russo, F. Finocchi and C. Noguera, Phys. Rev B **69**, 85411 (2004).

[19] H. J. Monkhorst and J. D. Pack, Phys. Rev. B **13**, 5188 (1976).

[20] X. Gonze and C. Lee, Phys. Rev. B **55**, 10355 (1997).

[21] X. Gonze, Phys. Rev. B **55**, 10337 (1997).

[22] M. Veithen, X. Gonze and Ph. Ghosez, Phys. Rev. B **66**, 235113 (2002).

[23] Ph. Ghosez and X. Gonze, J. Phys.: Condens. Matter **12**, 9179 (2000).

[24] X. Gonze, J. C. Charlier, D. C. Allan and M. P. Teter, Phys. Rev. B **50**, 13035 (1994).

[25] C. Lee and X. Gonze, Phys. Rev. B **51**, 8610 (1995).

[26] J. L. Feldman and D. J. Singh, Phys. Rev B **53**, 6273 (1996).

[27] Th. Schmidt, G. Kliche and H. D. Lutz, Acta Cryst. **C43**, 1678 (1987).

[28] J. O. Sofo and G. D. Mahan, Phys. Rev B **58**, 15620 (1998).

[29] D. J. Singh and W. E. Pickett, Phys. Rev B **50**, 11235 (1994).

[30] I. Lefebvre-Devos, M. Lassalle, X. Wallart, J. Olivier-Fourcade, L. Monconduit and J. C. Jumas, Phys. Rev B **63**, 125110 (2001).

[31] E. Z. Kurmaev, A. Moewes, I. R. Shein, L. D. Finkelstein, A. L. Ivanovskii and H. Anno, J. Phys.: Condens. Matter **16**, 979 (2004).

[32] T. Caillat, A. Borshchevsky and J.-P. Fleurial, J. Appl. Phys. **80**, 4442 (1996).

[33] E. Arushanov, M. Respaud, H. Rakoto, J. M. Broto and T. Caillat, Phys. Rev B **61**, 4672 (2000).

[34] J. Nagao, M. Ferhat, H. Anno, K. Matsubara, E. Hatta and K. Mukasa, Appl. Phys. Lett. **76**, 3436 (2000).

[35] B. C. Sales, D. Mandrus, B. C. Chakoumakos, V. Keppens and J. R. Thompson, Phys. Rev. B **56**, 15081 (1997).

[36] R. Resta, J. Phys.: Condens. Matter **14**, R625 (2002).

[37] G. S. Noals, G. A. Slack, D. T. Morelli, T. M. Tritt and A. C. Ehrlich, J. Appl. Phys. **79**, 4002 (1996).

[38] N. Marzari and D. Vanderbilt, Phys. Rev. B **56**, 12847 (1997).

[39] I. Souza, N. Marzari and D. Vanderbilt, Phys. Rev. B **65**, 035109 (2002).

[40] A. Kokalj, J. Mol. Graphics Modelling **17**, 176 (1999) [URL www.xcrysden.org].

[41] G. Kliche and H. D. Lutz, Infrared Phys. **24**, 171 (1984).

[42] X. Gonze, Ph. Ghosez, and R. W. Godby, Phys. Rev. Lett. **74**, 4035 (1995).

[43] S. Öğüt and K. M. Rabe, Phys. Rev B **54**, R8297 (1996).

[44] G. Kliche and W. Bauhofer, J. Phys. Chem. Solids **49**, 267 (1988).

[45] S. V. Dordevic, N. R. Dilley, E. D. Bauer, D. N. Basov, M. B. Maple and L. Degiorgi, Phys. Rev B **60**, 11321 (1999).

[46] C. Kittel, *Introduction to solid state physics*, (John Wiley & Sons, Inc., 1996).

[47] W. Zhong, R. D. King-Smith and D. Vanderbilt, Phys. Rev. Lett. **72**, 3618 (1994).

[48] W. A. Harrison, *Electronic Structure and the Properties of Solids*, (Freeman San Francisco, 1980).

[49] Ph. Ghosez, J.-P. Michenaud and X. Gonze, Phys. Rev B **58**, 6224 (1998).

[50] In Ref. 51, Lutz and Kliche report a value of 3.93 for $|Z^*_{Co}|$. However, they used a value of 10.84 for the optical dielectric constant to deduce $|Z^*_{Co}|$ from the LO-TO splitting of the infrared active phonons. This value has been corrected to 25.6 in a later work[41].

[51] H. D. Lutz and G. Kliche, Phys. Stat. Sol (b) **112**, 549 (1982).

[52] R. D. Shannon, Acta Cryst. **A32**, 751 (1976).

[53] G. S. Nolas and C. A. Kendziora, Phys. Rev B **59**, 6189 (1999).

[54] X. Gonze and C. Lee, Phys. Rev. B **55**, 10355 (1997).

[55] M. Veithen and Ph. Ghosez, Phys. Rev. B **65**, 214302 (2002).

[56] R. Hermann, private communication.

[57] J. Dong, O. F. Sankey and C. W. Myles, Phys. Rev. Lett. **86**, 2361 (2001).

[58] R. O. Pohl, Phys. Rev. Lett. **8** 481 (1962).

[59] G. S. Nolas, T. J. R. Weakley, J. L. Cohn and R. Sharma, Phys. Rev. B **61**, 3845 (2000).

[60] J. L. Cohn, G. S. Nolas, V. Fessatidis, T. H. Metcalf, and G. A. Slack, Phys. Rev. Lett. **82**, 779 (1999).